HIGH ENERGY GAMMA-RAY RADIATION ABOVE 300 keV ASSOCIATED WITH SOLAR ACTIVITY*

E. L. CHUPP, D. J. FORREST, and A. N. SURI
Dept. of Physics, University of New Hampshire, Durham, N.H. 03824 U.S.A.

Abstract. The present status of our knowledge concerning the production of gamma-ray lines and continuum during the impulsive phase of solar flares is reviewed. Our data in this field is based solely on the OSO-7 observations made in 1972, August 4 and August 7. The experimental data will be reviewed. These observations along with theoretical work of Ramaty and Lingenfelter (1973a, b) and the charged secondary observations of the Chicago group (Anglin *et al.*, 1973) lead to the investigation of different hypothetical models to explain the production of neutral and charged secondaries in the solar atmosphere. At the present time it is not possible to rule out the preflare and postflare accumulation models if all the data is considered. We will discuss the outstanding experimental questions to be answered in future investigations.

1. Introduction

The experimental investigations to detect solar neutrons and gamma rays which were reported in the literature by 1970, were reviewed previously by Chupp (1971). Up to that time there was no conclusive evidence for either solar neutron or gamma-ray fluxes. On the other hand, there were at least three highly disputed claims of observations of both solar neutrons and gamma-rays, all in times of modest or low solar activity. None of these 'possible' events occurred in coincidence with the optical phase in any flare. Nonetheless, since they are published as positive fluxes, we should keep the reports in mind and the conditions of solar activity under which they were observed. The Tata result of Apparao *et al.* (1966) was obtained under very quiet solar conditions; that of Daniel *et al.* (1967) was made several hours before a subflare. This result was seriously questioned by Holt (1967) since no neutron decay protons were seen by the OGO-A satellite which was in orbit at the time and should have seen them if the neutron flux was 10^{-1} neutrons $cm^{-2}\,s^{-1}$ as reported. This criticism has now been countered by Daniel *et al.* (1971) who have revised their result downward nearly an order of magnitude to 1.5×10^{-2} neutrons $cm^{-2}\,s^{-1}$ based on a new measurement of the atmospheric neutron flux which allowed them to convert the measured solar neutron counting rates to an absolute flux. In the case of gamma rays, Kondo and Nagase (1969) reported an extremely large (800%) increase in the gamma-ray flux (3–10 MeV) 10 min after a 1N flare and associated radio burst. The last positive report of gamma-ray increase was given by Hirasima *et al.* (1970), who reported a gamma-ray line flux coincident with a 1000 MHz radio burst. As satellite experiments in the future continue to search for gamma-ray and neutron events, it will be interesting to see if any enhancements are found under similar activity conditions as in the cases just discussed, then we can decide if indeed these peculiar observations are most

* Dr R. Ramaty was kind enough to present this paper in absence of all the authors.

Sharad R. Kane (ed.), Solar Gamma-, X-, and EUV Radiation, 341–359. All Rights Reserved.

probably positive or spurious. A detailed discussion of recent work and several other experiments may be found in Chupp *et al.* (1973).

II. OSO-7 Gamma-Ray Observations in August 1972

The only evidence we found for gamma rays associated with solar flares was during the August 4 and 7 events. No description of the University of New Hampshire OSO-7 instrument will be given here since this has been described thoroughly elsewhere (e.g. Higbie *et al.*, 1973; Chupp *et al.*, 1973).

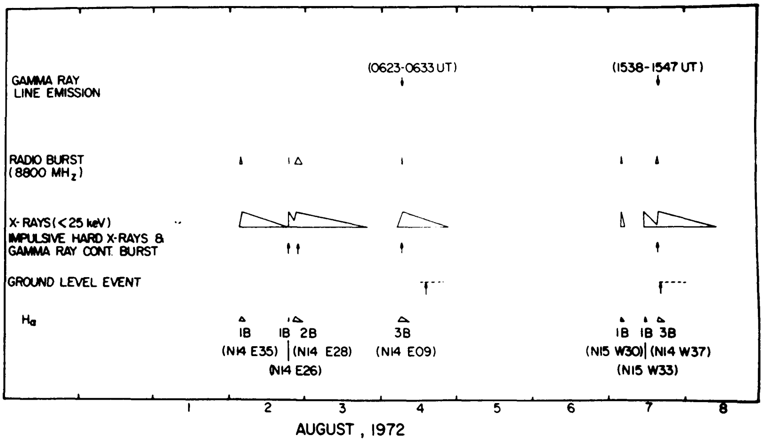

Fig. 1. Event chronology – August 1972.

Figure 1 shows a chronological history of several associated phenomena during the first two weeks of August 1972. As noted, gamma rays were observed during the beginning phase of the 0621 UT August 4 flare in close time association with a radio burst, an X-ray burst and the $H\alpha$ flash. In this case a ground-level cosmic-ray event was observed, delayed by $\sim$8 h from the flare. On August 7 gamma rays were observed after the maximum phase of the 1500 UT flare just after the satellite emerged into daylight.

(a) THE AUGUST 4 EVENT

The flare activity on August 4 started with a precursor flare in the X-ray band (0.5–3 Å) at 0507 UT (Dere *et al.*, 1973). The precursor activity continued for about an hour until 0610 UT when the main flare started in the X-ray band 7.5–15 keV as recorded by the UNH X-ray detector. The main optical flare started in Hα at $\sim$0621 UT. Before the OSO-7 satellite was eclipsed by the Earth at 0633.8 UT, excess gamma-ray line and continuum emission was recorded by the University of New Hampshire Gamma Ray Detector on OSO-7. Strong radio emission accompanied this event (Castelli *et al.*, 1973; Croom and Harris, 1973). There is very good correlation between the gamma ray continuum observed on OSO-7 and the impulsive radio emission

(Suri *et al.*, 1975). The onset as well as the time of maximum are the same within a minute.

Figures 2 and 3 show plots of the intensity-time profiles of the event in different X-ray and gamma-ray energy regions on a long and short time scale, respectively. The observational data is incomplete because of:

(1) Saturation in the lower 3 X-ray channels.

(2) Discontinuity in the data near the peak of the impulsive phase when the satellite was eclipsed by the Earth.

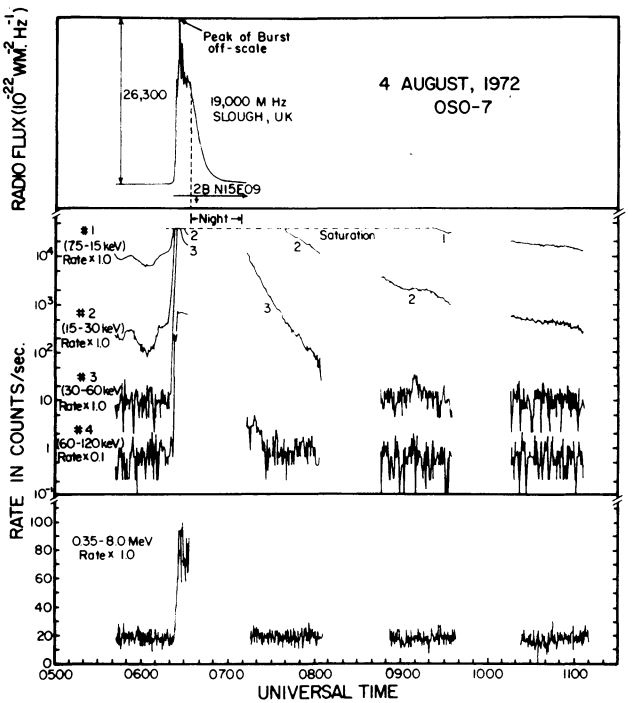

Fig. 2. Coarse time history – 1972, August 4; X-rays, γ-rays and radio emission.

It can be seen from Figure 3, however, that the X-ray flux increases approximately exponentially with time with an e-folding rise time, which decreased with increase in the X-ray energy. Also, the onset of the impulsive phase occurs earlier at lower X-ray energies.

(i) *Gamma-Ray Line Emission*

Figure 4 shows the time integrated solar and background gamma-ray counting rate spectrum accumulated during the time interval ~0624–0633 UT. The ordinate shows the total number of counts accumulated in each channel during the total live time of 91.4 s for the solar quadrant. The total number of counts in each channel up to channel 200 is shown and the sum of the counts in five consecutive channels there-

https://doi.org/10.1017/S0074180900071801 Published online by Cambridge University Press

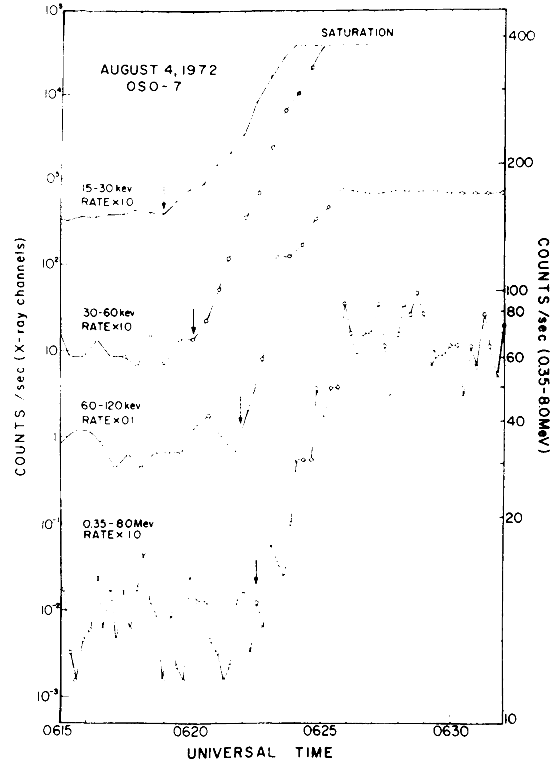

Fig. 3. Fine time history – 1972, August 4, X-rays, γ-rays.

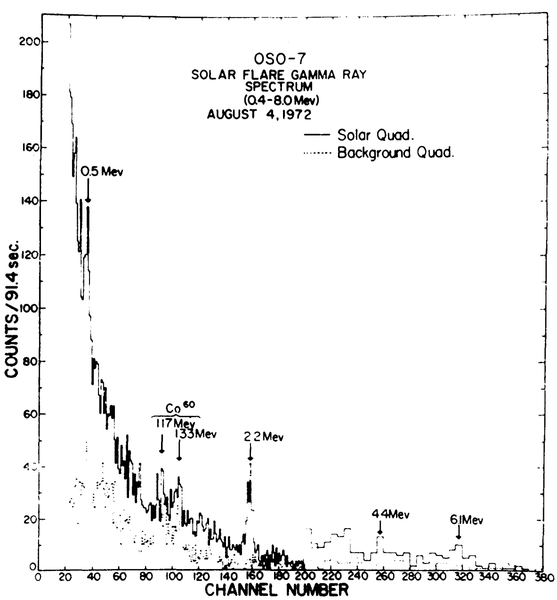

Fig. 4. Complete gamma-ray spectrum – 1972, August 4; 0624–0633 UT.

https://doi.org/10.1017/S0074180900071801 Published online by Cambridge University Press

after. The background spectrum has been normalized to the live time shown in the figure.

The flare spectrum shows a clear enhancement of the counting rate in both the 0.5 and 2.2 MeV spectral regions. The energy positions of these lines has been established from the calibration spectra and are at energies 510.7 ± 6.4 keV and at 2.24 ± 0.02 MeV. The 2.2 MeV line is about 15 σ above the continuum. The 0.5 MeV line is somewhat less significant but there is no question about its presence at about the 4 σ level. For the 0.5 MeV line a contribution in the background quadrant has been subtracted.

TABLE I

Flux Values for 1972, August 4 and 7

Time of flare observations	Gamma-ray flux at 1 AU (photons cm^{-2} s^{-1})			
3B (Hα) 1972, August 4, (0623:49–0633:02) UT Hα max – 0630 UT	510.7 ± 6.4 keV $(6.3 \pm 2.0) \times 10^{-2}$	2.24 ± 0.02 MeV $(2.80 \pm 0.22) \times 10^{-1}$	4.4 MeV $(3 \pm 1) \times 10^{-2}$	6.1 MeV $(3 \pm 1) \times 10^{-2}$
3B (Hα) 1972, August 7, (1538:20–1547:33) UT Hα max – 1530 UT	508.1 ± 5.8 keV $(3.0 \pm 1.5) \times 10^{-2}$	2.22 ± 0.02 MeV $(6.9 \pm 1.1) \times 10^{-2}$	4.4 MeV $< 2 \times 10^{-2}$	6.1 MeV $< 2 \times 10^{-2}$

The line features at 4.4 and 6.1 MeV are less significant ($\sim 3\,\sigma$) and do not stand by themselves. Their presence is indicated in Figure 4 because these are the most intense deexcitation lines from ^{12}C (4.4 MeV) and ^{16}O (6.1 MeV) and are expected to be produced in solar flares. Table I summarizes the excess average flux above the gamma-ray continuum in three full spectral scans for the four peaks mentioned above. The excess counting rates in the peaks were obtained by *first subtracting the background* quadrant counting rates from the solar quadrant counting rates and then fitting a function of the form

$$N(n) = A_1 + A_2 n + A_3 n^2 + B \exp[(n - n_0)^2 / 2\,\sigma^2] \qquad (1)$$

to the spectral data using 20–30 channels around the gamma-ray peak position. This function represents a Gaussian peak superimposed on a quadratic continuum.

The normalizing peak number B, the line widths, σ, and the parameters, A_1, A_2, and A_3 were varied to find the best fit as determined by a minimum in chi-square.

Table I also gives the flux values at the Earth for the spectral features at 4.4 MeV (^{12}C) and 6.1 MeV (^{16}O).

(ii) *Time Profiles of the Positron Annihilation and Neutron Capture Lines*

Figure 5 shows the intensity-time profiles of the 0.5 and 2.2 MeV lines observed during the impulsive phase of the August 4 event. The time resolution of the instrument (3 min) and poor statistics (particularly for the 0.5 MeV line) do not allow us

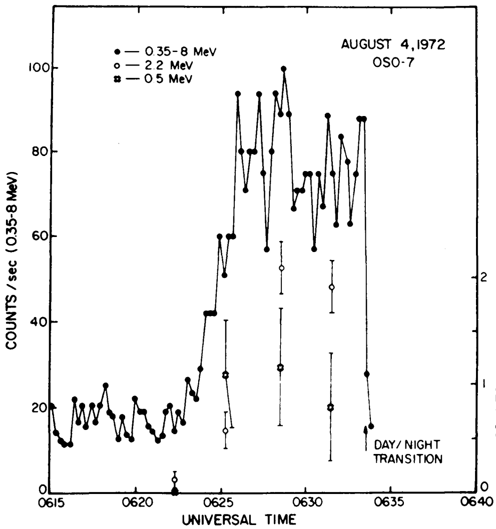

Fig. 5. Fine time history – 1972, August 4; 0.5 and 2.2 lines.

to draw any final conclusions about the history of the production of these lines. However, we can say that

(1) The production of these lines takes place in coincidence with the impulsive hard X-rays and gamma-ray continuum.

(2) The 0.5 and 2.2 MeV line radiation rises to its maximum values in 3–6 min. The observed time history of the 2.2 MeV line shows that a reasonable value of the capture time of the neutrons in the photosphere is 100 ± 50 s (Reppin *et al.*, 1973).

(iii) *Preflare Upper Limits*

According to the flare model proposed by Elliot (1969), the flare energy is stored as energetic protons in the flare region. These energetic protons acquire their energy through a slow acceleration process which could be operating at the flare site for hours or days. If this is the case, then a weak emission of gamma rays could be taking place in the flare region prior to the onset of a flare.

We have searched the data for gamma-ray line radiation prior to the start of the August 4 event. No evidence was found for the emission of 0.5, 2.2, 4.4, and 6.1 MeV lines during the period 1437–2110 UT on August 3 and 0540–0618 UT on August 4. Data were rejected during the time the spacecraft repeatedly went through the South Atlantic anomaly.

The 2 σ upper limit fluxes are given in Table II. The upper limit fluxes were obtained using the relation

$$F_\gamma \leqslant \frac{2\,\sigma}{S} \leqslant \frac{2}{S}\left[\frac{R_S}{T_S} + \frac{R_B}{T_B}\right]^{1/2} \tag{2}$$

where R_S is the counting rate during the period T_S when the detector was pointing at the Sun. S is the sensitivity for a particular gamma-ray line and R_B is the counting rate when the Sun was not in the field of view of the detector for a time T_B.

Since the background quadrant counting rate is contaminated with the atmospheric radiation when the solar quadrant contains the Sun, we have taken R_B to be the background quadrant counting rate during the satellite night (looking away from the Earth).

TABLE II

Upper limits on gamma-ray line emission prior to onset of the August 4 event (photons $cm^{-2}\ s^{-1}$)

0.5 MeV	2.2 MeV	4.4 MeV	6.1 MeV
$\leqslant 8.3 \times 10^{-3}$	$\leqslant 6.2 \times 10^{-3}$	$\leqslant 4.5 \times 10^{-3}$	$\leqslant 4.1 \times 10^{-3}$

(iv) *Shape of 0.5 MeV Line*

The possibility of observing thermal Doppler broadening in gamma ray lines produced during solar flares has been discussed by Kuzhevskii (1969) and Cheng (1972). The observation of these lines during the August 4 event allow us to put a limit on the temperature of the flare region in which these lines are produced.

Figure 6 shows the 0.5 MeV peak observed during the August 4 flare obtained by subtracting the background quadrant data from the solar quadrant data, and then subtracting a fit to the γ-ray continuum below the peak. The remaining peak was best

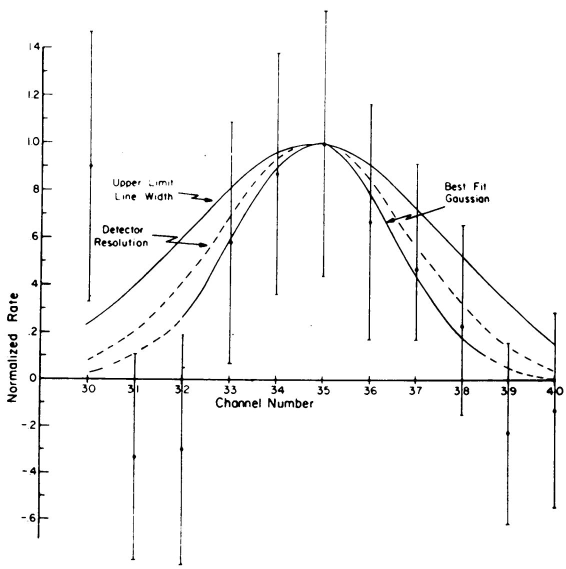

Fig. 6. Fit of excess counts to 0.51 MeV line – 1972, August 4.

https://doi.org/10.1017/S0074180900071801 Published online by Cambridge University Press

fitted by a Gaussian curve with a FWHM of 7.4%. The fact that the measured width (7.4%), within the uncertainty of the measurement, is the same as the expected width (8.8%), shows that there is no additional broadening of the positron annihilation line due to thermal effects. This gives an upper limit temperature in the flare region where annihilation takes place to be $< 1 \times 10^7$ K at a 3 σ confidence level.

(v) *Gamma-Ray Continuum*

In addition to the gamma-ray line emission, we also observed gamma-ray continuum emission extending up to 7 MeV as seen in Figure 4. The differential photon spectrum derived from Figure 4 along with that observed on TD-1A at lower energies (Van Beek, 1973) is shown in Figure 7. The spectrum shown was obtained by first subtracting the background quadrant counting rate spectrum from the solar quadrant counting rate spectrum. The counting rate contributions from gamma-ray lines at 0.5, 1.6, 2.2, 4.4, and 6.1 MeV were then subtracted including the Compton continuum at lower energies associated with the photopeaks. The photon spectrum incident on the detector was then found by transforming this counting rate spectrum, with the known line contributions removed, through the detector response by the 'strip-off' method (Burrus, 1960). The first step consisted of obtaining a reasonably accurate measure of the Compton continuum and of the first and second escape peaks for various energies of interest for the OSO-7 detector. Response function data collected by Higbie *et al.* (1973) at several energies were used for this purpose.

The Compton continuum correction was less than 20% of the observed counting rate at energies less than 0.7 MeV. However, the correction was about 30, 50, 44, 33, and 11 percent for energy bins 1–2, 2–4, 4–5, 5–6, and 6–6.5 MeV, respectively.

There are two effects which can give rise to the flattening of the observed gamma-ray continuum spectrum between 1–2 MeV. The first one is the Compton scattering of the 2.2 MeV upward moving photons in the photosphere which escape from the Sun. Wang and Ramaty (1974) have carried out Monte Carlo calculations on the transport of 2.2 MeV photons out of the photosphere and find that only a small fraction ($\sim 1\%$) of the observed flux between 1–2 MeV could be due to Compton scattering of 2.2 MeV photons in the photosphere.

The second effect is the Compton scattering of 2.2 MeV photons in the Earth's atmosphere. Because of the broad angular response ($\sim 100°$) of the instrument, it is likely that the detector registered scattered atmospheric radiation during a part of the event just prior to day/night transition when the Earth's atmosphere was in partial view of the detector. A detailed treatment of the problem is complicated; therefore, only a rough estimate of its effect on the observed continuum spectrum is made.

Considering the case of grazing incidence, we estimate that the flux of scattered photons in the energy range 1–2 MeV falling on the detector is 0.02 photons cm^{-2} s^{-1}. This is approximately 2% of the observed gamma-ray continuum flux between 1–2 MeV. It thus appears that the change in the spectral shape ~ 700 keV is real and not a local atmospheric effect.

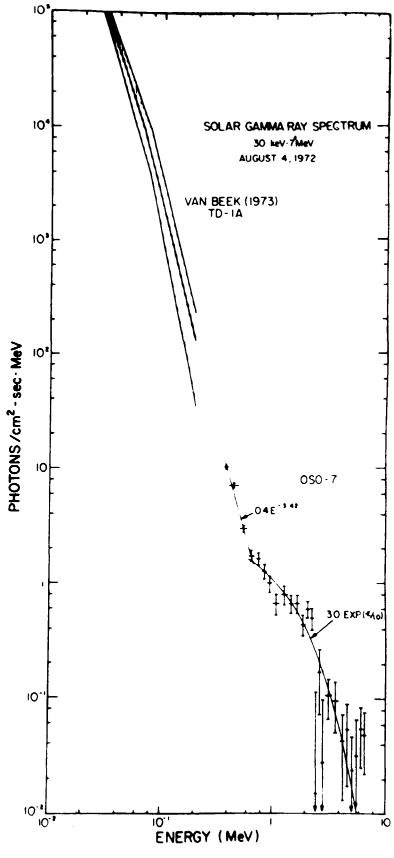

Fig. 7. Solar γ-ray continuum in 1972, August 4; 30 keV to 7 MeV.

In the energy range 360–700 keV, the differential photon spectrum in Figure 7 was fit to a power law

$$dJ/dE = 0.4\,E^{-3.42 \pm 0.3}\ \text{photons cm}^{-2}\,\text{s}^{-1}\,\text{MeV}^{-1} \tag{3}$$

by the least square method. For gamma-ray energies in the range 0.7–7 MeV, however, a single power law is a poor fit. In this energy range the data was fit by the weighted least squares method to an exponential of the form

$$dJ/dE = k_1 \exp(-E/E_0)\ \text{photons cm}^{-2}\,\text{s}^{-1}\,\text{MeV}^{-1}, \tag{4}$$

where $E_0 = (1.0 \pm 0.07)$ MeV.

In the energy range 30–203 keV, hard X-rays from this event were observed by the University of Utrecht detector on the TD-1A satellite (Van Beek, 1973; Van Beek *et al.*, 1973). The differential photon spectrum in the energy range 30–203 keV as observed on TD-1A is also shown in Figure 7.

The UNH X-ray data is not shown in Figure 7 because the X-ray detector saturated during the impulsive phase. The Utrecht detector on TD-1A did not saturate and also the pulse pile-up contamination is less than a few percent (Van Beek, 1973).

A power law spectrum of index 3.4 in the energy range 360–700 keV is consistent with the observations made from TD–1A at lower energies as shown in Figure 7. Over the energy range 29–203 keV, the TD-1A data (Van Beek, 1973) was fitted to a combination of two power law spectral distributions. Van Beek (1973) selected eight time intervals during the period 0623.5–0630.5 UT and determined parameters k and γ of the photon spectrum below and above the break. The spectral index varied from 2.7–3.5 below the break to 3.5–5.1 above the break. This is shown by the hatched area in Figure 7. The solid line in the hatched area represents the average spectral shape averaged over eight time intervals as given by Van Beek (1973).

The time averaged differential photon spectrum for the 1972, August 4 event over the energy range 30 keV–7 MeV shows two basic features:

(1) A change in the slope at 80–100 keV (Van Beek, 1973) when the power law spectral index changes from 3 to 3.9.

(2) A change in the spectral shape at $\sim$700 keV.

(b) AUGUST 7 EVENT

The August 7 event was the second large flare of the August solar activity that gave evidence for the emission of gamma-ray lines in the solar flares. The flare began in Hα at 1455 UT when the OSO-7 spacecraft was behind the Earth. Approximately 40 min after the onset of the flare, the spacecraft emerged into sunlight and enhanced

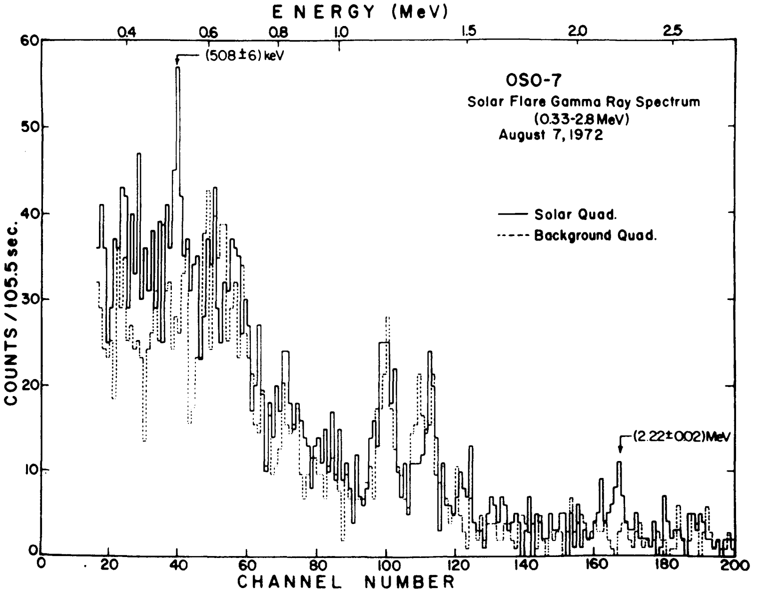

Fig. 8. Complete gamma-ray spectrum – 1972, August 7; 1538–1547 UT.

https://doi.org/10.1017/S0074180900071801 Published online by Cambridge University Press

counting rates in the spectral region around 0.5 and 2.2 MeV were observed. A final analysis of this data has not yet been completed so we will present only the preliminary results.

Figure 8 shows the solar and background spectra after the satellite emerged into daylight. Three full spectral scans are summed together covering the time interval from 1538.20–1547.33 UT. The lines at 0.5 and 2.2 MeV are the only lines clearly evident in the solar quadrant compared to the background quadrant. Table I gives a summary of the average gamma-ray line fluxes for the August 4 and 7 events.

III. Discussion and Interpretation of the August 1972 Solar Events

About seven years ago fairly detailed calculations carried out by Lingenfelter and Ramaty (1967) made predictions of the yield of the neutral secondaries at the Earth. In 1958, Severny predicted the production of neutrons associated with thermonuclear reactions occurring in shock fronts in the plasma associated with a solar flare, which could produce gamma rays from neutron-proton capture. Kuzhevskii (1969) has also made estimates of solar flare gamma-ray line fluxes.

Following the OSO-7 August 1972 observations, Ramaty and Lingenfelter (1973a, b) have extensively revised their calculations and this work provides the main basis on which interpretation can be made. It should be noted, however, that there is no complete geometrical flare model available at this time with which one can make more refined calculations.

The calculations of Lingenfelter and Ramaty (1967) and Ramaty and Lingenfelter (1973a, b) make the basic assumption that the differential spectrum of charged particles at the Sun is of the form $\mathrm{d}N/\mathrm{d}P \propto \exp(-P/P_0)$. The parameter P_0 determines whether the spectrum is a relatively hard or soft spectrum of charged particles. Ramaty and Lingenfelter have used the basic cross sections that are available in the literature and inferred ones when no experimental values are available.

Gamma ray yields have been calculated for a variety of production modes as shown in Table III. The yields of gamma rays have been calculated for two cases:

(1) The thick-target case, which assumes that the accelerated particles are undergoing nuclear interactions as they slow down and stop in sufficiently dense solar atmosphere. For example, in neutral hydrogen the amount of matter required to stop a 50 MeV proton is 1 gm cm^{-2}.

(2) The thin-target case, which assumes that the spectrum of charged particles is not modified as nuclear interactions are taking place. This means that the path length or amount of matter traversed by the particles is small compared with their nuclear interaction length or that ionization energy loss is just balanced by the gain in energy from a 'continuously' operating acceleration process.

These calculations also make the implicit assumption that in the thin target case the whole process is isotropic. This point is important when considering the production of high energy neutrons (> 50 MeV) and π^0 mesons which preserve the momentum of the incident charged particles. Therefore, the neutrons in the first case may be emitted in a highly anisotropic manner from the Sun (see Chupp, 1971). Detection of these radiations at the Earth may be difficult, therefore, if the charged-particle acceleration process is highly anisotropic at the Sun.

The lower energy gamma rays listed in Table III should all be isotropically emitted independent of the angular distribution of the incident charged particles. The strong magnetic fields in flare regions might conceivably produce some effects on these lower energy gamma rays, but this refinement has not been made in the Ramaty and Lingenfelter calculations.

TABLE III

Gamma-ray line emission mechanisms from Ramaty and Lingenfelter (1973a)

Photon energy (MeV)	Origin	Production mode
0.511	Positron annihilation	$e^{+}+e^{-}\rightarrow 2\gamma$
2.23	Deuterium de-excitation following neutron capture	$H'+n\rightarrow H^{2}+\gamma$
1.63	$Ne^{20\,(1.63)}$ deexcitation	Ne^{20} (p, p′) $Ne^{20(1.63)}$
	$N^{14(3.94)}=N^{14(2.31)}$ de-excitation	N^{14} (p, p′) $N^{14(3.94)}$
2.31	$N^{14(2.31)}$ de-excitation	N^{14} (p, p′) $N^{14(2.31)}$
		N^{14} (p, p′) $N^{14(3.94)}\rightarrow N^{14(2.31)}$
		N^{14} (p, n) $O^{14}\rightarrow N^{14(2.31)}$
4.43	$C^{12(4.43)}$ de-excitation	C^{12} (p, p′) $C^{12(4.43)}$
		O^{16} (p, pα) $C^{12(4.43)}$
5.2	$O^{15(5.20)}$ de-excitation	O^{16} (p, pn) $O^{15(5.20)}$
	$N^{15(5.28)}$ de-excitation	O^{16} (p, 2p) $N^{15(5.28)}$
6.14	$O^{16(6.14)}$ de-excitation	O^{16} (p, p′) $O^{16(6.14)}$
7.12	$O^{16(7.12)}$ de-excitation	O^{16} (p, p′) $O^{16(7.12)}$

We will not describe in further detail here the Ramaty and Lingenfelter calculations, but will show how these have been used to interpret the OSO-7 observations described above. Shown in Figure 9 is the theoretical ratio of a given gamma ray yield to the theoretical yield of 2.2 MeV gamma rays plotted versus the characteristic rigidity P_0 of the charged particles spectrum for a thick-target interaction model. The broad horizontal bands shown in the graph correspond to the experimentally measured OSO-7 gamma-ray flux ratios at the indicated energies with associated statistical errors in the flux measurements for the August 4 event.

The corresponding curve for the thin-target interaction model is shown in Figure 10. From either Figure 9 or Figure 10, it can be seen that a characteristic rigidity of the protons at the Sun of the order 70–100 MV is required to obtain a consistency for the observed ratio for all the measured gamma-ray yields. Recent slight modifications in the calculations and the experimental results do not change this conclusion*.

This range of P_0's agrees reasonably well with that deduced by Ramaty and Lingenfelter from the protons observed near the Earth by various spacecraft (cf. Kohl *et al.*, 1973). Thus, the gamma ray observations and the particle observations support the view that the August 4 flare was relatively soft in terms of accelerated particle energies.

* See notes added in proof.

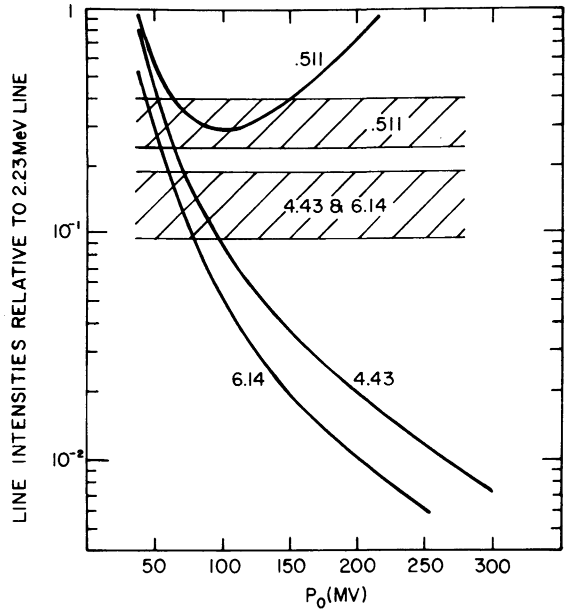

Fig. 9. Theoretical relative intensity of γ-ray line flux relative to the 2.2 MeV theoretical flux in thick-target geometry and compared with experimental results.

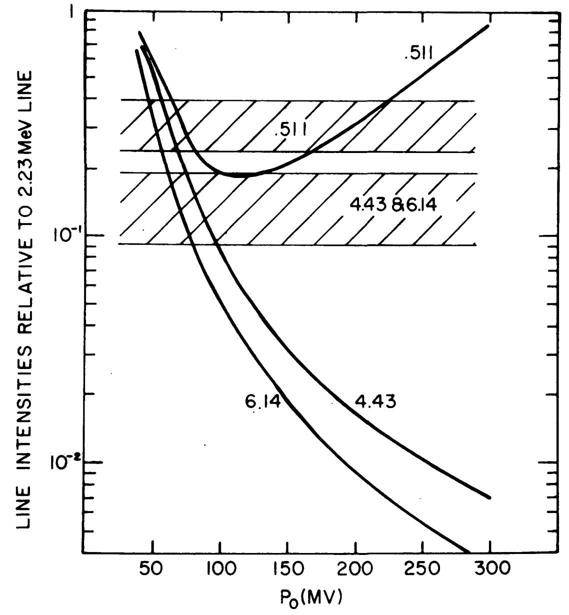

Fig. 10. Theoretical relative intensity of γ-ray line flux relative to the 2.2 MeV theoretical flux in thin-target geometry and compared with experimental results.

https://doi.org/10.1017/S0074180900071801 Published online by Cambridge University Press

On the other hand, Pomerantz and Duggal (1973) have given evidence for a harder component (associated with the 0621 flare), which produced a ground-level cosmic-ray event some 6 h later; however, no excess solar gamma rays were seen at that time. This observation is one of the major anomalies associated with the August 4 events.

A further interesting consideration has recently been raised with regard to the line at 0.5 MeV observed on August 4. This concerns the question of whether or not the positron annihilation takes place through free annihilation or through the bound state of positronium. In the former case, a 2-photon annihilation is the most predominant gamma-ray spectrum seen and gives the sharp line at 0.5 MeV. On the other hand, if annihilation occurs through the bound state, both 2-photon annihilation through the singlet state of positronium and 3-photon annihilation through the triplet state of positronium can take place. In the latter case, the gamma-ray spectrum is not a single line spectrum, but it is a continuous spectrum extending from the 0.5 MeV line downward. Leventhal (1973), in connection with the study of positron annihilation in a low density astrophysical medium where the atomic density is less than 10^{15} atoms cm^{-3}, points out that the continuum gamma-ray spectrum resulting from annihilation through the bound state of positronium could be predominant. If one is using a detector with relatively poor energy resolution, the apparent peak position of the 0.5 MeV line can be shifted to a lower energy as a result of the folding of the instrument resolution in with the triplet continuum spectrum and singlet positronium line spectrum.

As noted earlier, the energy of the 0.5 MeV line corresponds to 0.51 MeV within an error of ~ 5 keV. Annihilation through positronium formation could shift our photopeak to a lower limit of about 505 keV within our error. Thus one cannot conclude absolutely from this that there is not some positronium formation present in the spectrum observed. The shape of the 0.5 MeV line has been carefully studied and it is concluded that there is no asymmetry observable on the low energy side. This allows us to state that we are 99% certain that the annihilation spectrum we see is not a result of 100% positronium formation. Poor statistics does not allow putting a specific limit on the amount of P_s. Thus collisional breakup of the positronium at $n_{\mathrm{atomic}} > 10^{15}\ \mathrm{cm}^{-3}$ is possible, or the triplet P_s state is quenched by strong magnetic fields, or the P_s formation rate is reduced by flare temperatures greater than 7×10^5 K as suggested by Ramaty and Lingenfelter (1973b). Thus presumably we are looking here at a free annihilation spectrum; however, the limited statistics do not permit a definitive answer to this interesting question.

A definite resolution of this question will undoubtedly require observations with solid-state detectors. It is perhaps worth noting that there are many ways of quenching the triplet state of positronium, such as strong magnetic fields in the flare for the $m=0$ state.

Since the line width shows no broadening beyond what is expected from the measured detector resolution, one is able to place an upper limit on the temperature of the annihilation region by considering a maximum width based on the error in our resolution measurements. This point was discussed above under the experimental observations. From the experimental observation that the 0.51 MeV line was evident within 200 s of the flare onset, the electron density in the annihilation region must be $\gtrsim 10^{12}$ electrons cm^{-3} since the mean capture time is $\propto n_e^{-1}$.

Wang and Ramaty (1974) have recently carried out a detailed study on the time history of neutrons produced in nuclear reactions above the solar photosphere. Using Monte Carlo calculations they explore the fate of mono-energetic groups of neutrons produced isotropically, half of which go into the photosphere. This work takes into account several factors which include an ambient $^3He/H$ ratio of the solar photosphere, the radioactive decay of neutrons, the escape of neutrons directly to the Earth, and the escape of neutrons which scatter in the photosphere and then leave the Sun.

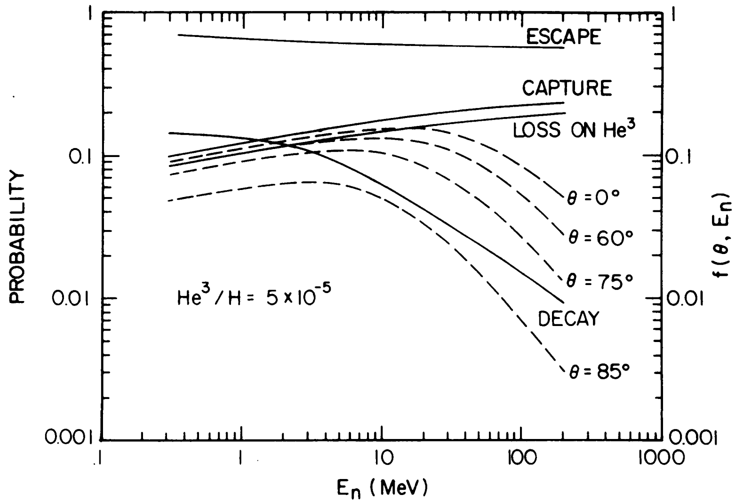

Fig. 11. Neutron fate in the photosphere versus neutron energy on left ordinate. On right ordinate, the probability of escape of the 2.2 MeV gamma ray vs. neutron energy and different angles of emission.

They then calculate the capture of neutrons on protons to give the yield of 2.2 MeV gamma rays taking into account the Compton scattering of the photons as they leave the region of capture. The loss of neutrons in capture on ^3He could reduce the predicted 2.2 MeV line intensity. The resulting Mont Carlo probabilities for the neutrons and the relative photon yields for various initial neutron energies are shown in Figure 11, which shows the case when the $^3He/H$ abundance is 5×10^{-5}. At low neutron energies and for an emission angle of gamma rays relative to the solar vertical given by the angle θ, the relative photon yield per neutron is close to the neutron capture probability on protons. This means that gamma rays from low energy neutrons observed close to the vertical, escape essentially unattenuated from the Sun. At higher energies and at larger angles; however, there is a significant attenuation of the gamma rays. In the previous Lingenfelter and Ramaty (1967) calculations, it was assumed that all downward moving neutrons are captured and all upward moving photons escape from the Sun. In this case the relative gamma flux per neutron should be $\frac{1}{2}$.

https://doi.org/10.1017/S0074180900071801 Published online by Cambridge University Press

However, from Figure 11 we see that depending on the energy of the neutrons, the location of the flare of the Sun, which determines the angle θ and the amount of the ^{3}He in the photosphere, one can overestimate the gamma yield by at least a factor of 2.5. Furthermore, if the flare occurs close to the limb of the Sun, the 2.2 MeV line could become essentially unobservable. For such limb flares the 0.5 MeV line and the nuclear de excitation lines would still be observable if these lines are produced above the photosphere. The August 4 flare was near the central meridian $\theta \sim 0$.

In case the ^{3}He/H ratio is zero, the relative gamma yields rise as also shown by Wang and Ramaty (1974). A basic result of these new detailed Monte Carlo calculations on the fate of neutrons produced in solar nuclear reactions is to reduce the calculated 2.2 MeV gamma-ray flux at the Earth from isotropically emitted neutrons from 50% to 20% depending upon the ^{3}He abundance as well as the angle or the amount of photospheric material. The time history of the 2.2 MeV line is also determined in these new calculations for each neutron energy. These Monte Carlo calculations will be valuable in the future when experiment and theory lead us to a more detailed acceleration model which gives the spectrum and time history of the solar cosmic rays at the Sun. These calculations also suggest that a limit may be placed on the ^{3}He/H abundance.

There are two other important considerations relating to these gamma-ray measurements. One point is concerned with the absolute number of protons required at the Sun in order to produce the observed yield of gamma rays at the Earth. The other is to take into account the observations on the charged secondary particles such as ^{3}He, deuterons, and triton nuclei, which are produced in similar nuclear reactions and observed at the space probes Pioneer 9 and 10 (by the University of New Hampshire and GSFC groups) and the IMP satellites 4, 5, and 6 (Anglin *et al.*, 1973). On the first point, there is a possibility of a discrepancy between the number of protons (>30 MeV) required at the Sun to produce the August 4 gamma-ray lines and the number of protons seen at the Earth by various spacecraft. There may be 10–10^3 more protons observed near the Earth than required at the Sun as discussed by Ramaty and Lingenfelter (1973a, b) and Forrest *et al.* (1974). On the second point, Forrest *et al.* (1974) have argued that if one takes into account the ^{3}He secondary production observed by Pioneer 10 as well as the gamma-ray observations, then ~ 1 gm cm^{-2} of solar material must be traversed in order to explain both the charged secondary and the gamma-ray yields.

Another model that must be considered is the preflare acceleration model, such as envisioned by Elliot (1973) in which the solar cosmic-ray particles are accelerated over a long period of time of the order of days in a relatively thin solar atmosphere, and the flare phenomena is a manifestation of the release of these particles. The observed gamma rays could be produced in a thick target situation with the ^{3}He and other charged secondaries having been produced prior to the flare but released at the time of the impulsive flare. A density of 10^6–10^7 particles cm^{-3} in the solar atmosphere would be the medium in which such preflare acceleration could occur. This particle density is constrained by the total number of SCR for a thin-target situation and the absence of an observable preflare gamma-ray flux. The time required in order to integrate a path length of 1 g cm^{-2} amounts to something of the order of 10–100 days. This is too long a time because the drift of the charged particles across magnetic field lines would undoubtedly release them from any reasonable size trapping region. Clearly, the detailed understanding of the solar cosmic rays and the secondary yields of positrons and neutrons giving the gamma rays and the charged He, D, and T isotopes is in too primitive a state in order to completely determine a model at this time.

Most of the reactions producing gamma-ray lines that have been considered in the theoretical calculations have been due to direct proton reactions on ambient solar nuclei or reactions of protons or α particles producing neutrons, π^+ and π^0 mesons, and β^+ emitters which eventually give rise to the 2.2 MeV gamma ray, the 0.51 MeV gamma ray, and π^0 decay gammas of average energy 70 MeV. Recently Kozlovsky and Ramaty (1974) have considered production of gamma-ray lines by α–α reactions. In particular the following two reactions can produce lines at 431 keV and 478 keV.

$$\begin{array}{ll} {}^4\mathrm{He}(\alpha, \mathrm{n})\,{}^7\mathrm{Be}^* & 431\ \mathrm{keV} \\ {}^4\mathrm{He}(\alpha, \mathrm{n})\,{}^7\mathrm{Be} \xrightarrow[\varepsilon]{12\%} {}^7\mathrm{Li}^* & 478\ \mathrm{keV} \\ {}^4\mathrm{He}(\alpha, \mathrm{p})\,{}^7\mathrm{Li}^* & 478\ \mathrm{keV} \end{array} \tag{5}$$

The first two reactions have thresholds at 9.7 MeV nucleon^{-1} and 8.5 MeV nucleon^{-1}, respectively, and the last reaction has a threshold at 8.5 MeV nucleon^{-1}. Kozlovsky and Ramaty argue that the cross-sections of all these reactions is ~ 100 mb at 10 MeV nucleon^{-1} and that the production cross-section of ^{7}Be in the ground state and first excited states are the same. They conclude that the intensities of these two lines from α–α reactions in solar flares should be as large or larger than the intensities of the 4.43 MeV line oı 6.14 MeV line. Even though the OSO-7 flare spectrum on August 4 shows a suggestion of features at about the channels corresponding to 431 keV, they are not statistically significant. The question will have to be resolved by future gamma-ray experiments.

IV. Summary and Conclusions

We list in Table IV a summary of the principal conclusions that can be made from the gamma ray observations on August 4.

The OSO-7 observations give evidence for the emission of gamma-ray lines in only two of the largest flares of the August 1972 series. Therefore, the most critical need for future experiments is to make more frequent measurements and with higher sensitivity instrumentation in order to obtain the time history of the gamma-ray lines, especially those from de-excitation of excited nuclei in C, N, O, etc. In addition, gamma-ray detectors of much higher energy resolution are needed in order to fully investigate the line shapes of the gamma-ray lines that are produced so the positronium question can be studied and possible Doppler broadening and Doppler shifts determined.

TABLE IV

Principal conclusions from gamma-ray observations in 1972, August 4

Gamma-ray producing nuclear reactions begin in the first 200 s with the hard X-ray and before the optical maximum.
Nuclear reactions occur for $\geqslant 600$ s.
Density of annihilation region $\gtrsim 10^{12}$ (elec cm^{-3}).
Temperature in $e^+ + e^- \to 2 \to 3\ \gamma$ region $< 10^7$ K.
Low-energy primary spectrum at Sun for gamma-ray production consistent with prompt low-energy spectrum seen at Earth and in space.
Total particle energy in thick target dump $< 10^{28}$ erg.

Acknowledgements

This work was supported by NASA under Contract Nas 5-11054 and NGR 30-002-021. We are thankful for the contributions of several persons in the fabrication and data analysis phase of the experiment, particularly Dr P. Higbie, A. A. Sarkady, I. U. Gleske, S. Foss, Sue Croteau, Margaret Simmons, Kishore and Dipika Patel, P. Ferguson, P. Dunphy and Dr C. Reppin. We also express our appreciation to Mary Miklos Chupp for editing the manuscript.

Notes added in proof: Some further revisions in the theoretical results shown in Figures 9 and 10 have been made by Ramaty and Lingenfelter (1975) and are discussed in another paper in this volume (page 363). These new calculations indicate that the characteristic rigidity P_0 for an exponential rigidity spectrum can nominally range from ~ 100–150 MV depending on thick or thin target assumptions, respectively. The experimental results can also be reconciled with a differential power law spectrum of form $E^{-\alpha}$ with the exponent ranging nominally from 2–3 depending on thin or thick target assumptions, respectively.

References

Anglin, J. D., Dietrich, W. F., and Simpson, J. A.: 1973, in R. Ramaty and R. G. Stone (eds.), *Symposium on High Energy Phenomena on the Sun*, NASA SP-342, p. 315.

Apparao, M. V. K., Daniel, R. R., Vijayalakshmi, B., and Bhatt, V. L.: 1966, *J. Geophys. Res.* **71**, 1781.

Burrus, W. R.: 1960, *IRE Trans. Nucl. Sci.* NS-7, 102.

Castelli, J. P., Barron, W. R., and Badillo, V. L.: 1973, World Data Center A, *Report UAG* **28**, Part 1, 183.

Cheng, C. C.: 1972, *Space Sci. Rev.* **13**, 3.

Chupp, E. L.: 1971, *Space Sci. Rev.* **12**, 486.

Chupp, E. L., Forrest, D. J., and Suri, A. N.: 1973, in R. Ramaty and R. G. Stone (eds.), *Symposium on High Energy Phenomena on the Sun*, NASA SP-342, p. 285.

Croom, D. L. and Harris, L. D. J.: 1973, World Data Center A, *Rept. UAG* **28**, Part 1, 210.

Daniel, R. R., Joseph, G., Lavakare, P. J., and Sunderrajan, R.: 1967, *Nature* **213**, 21.

Daniel, R. R., Gokhale, G. S., Joseph, G., and Lavakare, P. J.: 1971, *J. Geophys. Res.* **76**, 3152.

Dere, K. P., Horan, D. M., and Kreplin, R. W.: 1973, World Data Center A, *Rept. UAG* **28**, Part 2, 298.
Elliot, H.: 1969, in C. de Jager and Z. Švestka (eds.), *Solar Flares and Space Research*, North-Holland Publ. Co., Amsterdam, p. 356.
Elliot, H.: 1973, in R. Ramaty and R. G. Stone (eds.), *High Energy Phenomena on the Sun*, NASA SP-342, p. 12.
Forrest, D. J., Chupp, E. L., Suri, A. N., and Dunphy, P.: 1974, *Bull. Amer. Phys. Soc.* **19**, 458.
Higbie, P. R., Chupp, E. L., Forrest, D. J., and Gleske, I. U.: 1972, IEEE Trans. Nucl. Sci., *NS-19*, 606.
Higbie, P. R., Forrest, D. J., Gleske, I. U., Chupp, E. L., and Burtis, D. W.: 1973, *Nucl. Instrum. Methods* **108**, 167.
Hirasima, Y., Okudaira, K., and Yamagami, T.: 1970, *Acta Phys. Hung.* **29**, Suppl. 2, 683.
Holt, S. S.: 1967, *J. Geophys. Res.* **72**, 3507.
Kohl, J. W., Bostrom, C. O., and Williams, D. J.: 1973, World Data Center A, *Rept. UAG* **28**, Part 2, 330.
Kondo, I. and Nagase, F.: 1969, in C. de Jager and Z. Švestka (eds.), *Solar Flares and Space Research*, North-Holland Publ. Co., Amsterdam, p. 134.
Kozlovsky, B. and Ramaty, R.: 1974, *Astrophys. J. Letters* **191**, L43.
Kuzhevskii, B. M.: 1969, *Soviet Astron. – AJ* **12**, 595.
Lingenfelter, R. E. and Ramaty, R.: 1967, in B. S. P. Shen (ed.), *High Energy Nuclear Reactions in Astrophysics*, W. A. Benjamin Press, New York, p. 99.
Levanthal, M.: 1973, *Astrophys. J. Letters* **183**, L147.
Pomerantz, M. A. and Duggal, S. P.: 1973, World Data Center A, *Rept. UAG* **28**, Part 2, 430.
Ramaty, R. and Lingenfelter, R. E.: 1973a, in R. Ramaty and R. G. Stone (ed.), *High Energy Phenomena on the Sun*, NASA SP-342, p. 301.
Ramaty, R. and Lingenfelter, R. E.: 1973b, *Proc. 13th International Cosmic Ray Conf.*, Denver, Colo., **2**, 1590.
Ramaty, R. and Lingenfelter, R. E.: 1975, this volume, p. 363.
Reppin, C., Chupp, E. L., Forrest, D. J., and Suri, A. N.: 1973, *Proc. 13th International Cosmic Ray Conf.*, Denver, Colo., **2**, 1577.
Severny, A. B.: 1958, *Soviet Astron. – AJ* **2**, 310.
Suri, A. N., Chupp, E. L., Forrest, D. J., and Reppin, C.: 1975, submitted for publication.
Van Beek, H. F.: 1973, Ph.D. Thesis, Physics Dept., Univ. of Utrecht, Holland.
Van Beek, H. F., Hoyng, P., and Stevens, G. A.: 1973, World Data Center A, *Rept. UAG* **28**, Part 2, 319.
Wang, H. T. and Ramaty, R.: 1974, *Solar Phys.* **36**, 129.